Steel and Composite Structures, *Vol. 18, No. 5 (2015) 1239-1258*
DOI: http://dx.doi.org/10.12989/scs.2015.18.5.1239

Simulating the construction process of steel-concrete composite bridges

Jie Wu [*1], Dan M. Frangopol [2a] and Mohamed Soliman [2b]

[1] *Department of Building Engineering, Tongji University, 1239 Siping Road, Shanghai 200092, PR China*
[2] *Department of Civil and Environmental Engineering, ATLSS Engineering Research Center, Lehigh University, 117 ATLSS Drive, Bethlehem, PA 18015-4729, USA*

(*Received May 14, 2014, Revised November 08, 2014, Accepted November 15, 2014*)

Abstract. This paper presents a master-slave constraint method, which may substitute the conventional transformed-section method, to account for the changes in cross-sectional properties of composite members during construction and to investigate the time-dependent performance of steel-concrete composite bridges. The time-dependent effects caused by creep and shrinkage of concrete are considered by combining the age-adjusted effective modulus method and finite element analysis. An efficient computational tool which runs in AutoCAD environment is developed to simulate the construction process of steel-concrete composite bridges. The major highlight of the developed tool consists in a very convenient and user-friendly interface integrated in AutoCAD environment. The accuracy of the proposed method is verified by comparing its results with those provided by using the transformed-section method. Furthermore, the computational efficiency of the developed tool is demonstrated by applying it to a steel-concrete composite bridge.

Keywords: steel-concrete composite bridge; simulation; construction; master-slave constraint; AutoCAD; creep; shrinkage

1. Introduction

During the past two decades, rapid developments in the design, construction, and maintenance technologies of steel-concrete composite bridges have occurred. Since the steel provides high tensile capacity and the concrete possesses the adequate compressive strength, these bridges are usually characterized by high strength, full usage of materials, high stiffness, and sufficient ductility. However, the structural behavior of the steel-concrete composite bridges is complex due to the different material properties of steel and concrete. Especially, the time-dependent behavior of concrete, such as creep and shrinkage, makes it difficult to evaluate the long-term structural response of this type of bridges.

Many studies have focused on the evaluation of the creep and shrinkage behavior of concrete (Bažant 1972, 2001). Moreover, the time-dependent behavior of steel-concrete composite beams

*Corresponding author, Associate Professor, E-mail: wwujie@tongji.edu.cn
[a] Professor, E-mail: dmf206@lehigh.edu
[b] Research Associate, E-mail: mos209@lehigh.edu

http://www.techno-press.org/?journal=scs&subpage=8 ISSN: 1229-9367 (Print), 1598-6233 (Online)

has been investigated by several researchers. Gilbert (1989) compared two alternative methods, namely the Age-adjusted Effective Modulus Method (AEMM) and the Rate of Creep Method (RCM), for the time-dependent analysis of composite steel-concrete sections, and provided two procedures for hand calculations. Amadio and Fragiacomo (1997) presented a simplified approach to evaluate creep and shrinkage effects in a steel-concrete composite beam with rigid or deformable connections based on the AEMM method. Tehami and Ramdane (2009) presented a creep analytical model of a composite steel-concrete section which does not require an incremental calculation. Nevertheless, most studies in this field focused on the analysis of the long-term behavior at the serviceability limit state (Fragiacomo *et al*. 2004, Jurkiewiez *et al*. 2005, Amadio *et al*. 2012). Few investigators studied the effects of the construction process on the behavior of steel-concrete composite bridges. Kwak *et al*. (2000) developed a model using a layer method to determine the equilibrium conditions in a cross-section, and evaluated the effects of the slab casting sequences. Mari *et al*. (2003) studied the influence of the construction process on the structural behavior of composite bridges, and reported that the most suitable construction solution depends on the most restrictive design criterion of the project. Dezi and Gara (2006) proposed a model for the analysis of the construction sequences of steel-concrete composite decks in which the slab is cast-in-situ in segments, and the numerical solution is obtained by means of a step-by-step procedure and the finite element method.

During the construction of steel-concrete composite bridges, since the new concrete slab segments are usually poured after the steel girder has been assembled, the resisting cross-sections of composite members may change at different construction stages, and these changes must be considered in the construction simulation of this structure. Currently, there are mainly three methods to handle the analysis of composite sections: the transformed-section method (Gilbert 1989, Gilbert and Bradford 1995), the discrete-section method (Mari *et al*. 2003, Liu *et al*. 2012), and the separated-section method (Amadio and Fragiacomo 1997, Fragiacomo *et al*. 2004, Dezi and Gara 2006, Pedro and Reis 2010). In the transformed-section method, the components of the cross-section of a composite member are transformed into equivalent steel or concrete ones based on the material properties. The discrete-section method divides the cross-section into several areas (e.g., layers or fibers) and computes the properties of the element by integrating these areas during numerical analysis. In the separated-section method, the steel and concrete parts of the composite member are divided into several separated elements which are connected with rigid or spring links. Since it may be difficult, in the development process of the computational tool, to deal with the changes of cross-sectional properties in construction process by using the transformed-section method or the discrete-section method, the separated-section method is selected in this paper and used in the developed tool.

Nowadays, the finite element method has become a widely accepted tool for structural analysis. General commercial finite element software packages, such as ABAQUS (2010) and ANSYS (2012), have been developed to solve various structural engineering problems. In order to use such software packages to simulate the construction process of steel-concrete composite bridges, one must perform significant work regarding the modeling of the structure. Furthermore, the constitutive models of creep in such software are mainly used for metallic or rock-soil materials, not for concrete. For the purpose of calculating the effects of concrete creep, one needs to create the creep model by setting several parameters obtained via numerical simulations. Thus, their use may be difficult for most engineers. Therefore, it is necessary to develop a computational tool with a user-friendly convenient interface, to simulate the construction process of steel-concrete composite bridges.

This paper presents a master-slave constraint method to model the construction process and to investigate the time-dependent performance of Steel-Concrete Composite Bridges. An efficient computational tool, named SCCB, is developed to simulate the construction process of these bridges. The creep and shrinkage of concrete are considered by combining the AEMM method and finite element analysis. The accuracy of the proposed method is verified by comparing its results with those of the transformed-section method. The major highlight of the developed tool is that it has a user-friendly interface and it is very convenient to use since it is integrated in the AutoCAD environment.

2. Finite element formulation and mathematical model

2.1 Finite element formulation

During the construction process of steel-concrete composite bridges, the longitudinal construction scheme, the cross-sectional properties, the applied loads, and the support conditions may change. These changes can be simulated with finite element analysis by activating or deactivating elements, loads, and restraints at different construction stages. The formulation for the construction process simulation can be written as

$$\left[{}^{i}K\right]\{\Delta u\} = {}^{i}Q - \left[{}^{i-1}F\right] \tag{1}$$

where superscripts i and $i-1$ are the stage indices; $[{}^{i}K]$ is the stiffness matrix at the ith stage; ${}^{i}Q$ is the external load vector at the ith stage; $[{}^{i-1}F]$ is the internal force vector computed from stresses at the $(i-1)$th step; and $\{\Delta u\}$ is the vector of incremental displacements.

Eq. (1) can be solved starting from the first construction stage to the last one, and then the nodal displacements and element force can be obtained by using the principle of superposition.

2.2 Shrinkage and creep model

The main shrinkage and creep models of concrete include the ACI209 model (Bažant 1988), CEB-FIP model (1990), B3 model (Bažant 1995) and GL2000 model (Gardner and Lockman 2001). The CEB-FIP model (1990), adopted in this paper, expresses the total shrinkage strains $\varepsilon_{cs}(t, t_s)$ as

$$\varepsilon_{cs}(t, t_s) = \varepsilon_{cso}\beta_s(t - t_s) \tag{2}$$

with

$$\beta_s(t - t_s) = \left[\frac{(t - t_s)/t_1}{350(h/h_0)^2 + (t - t_s)/t_1}\right]^{0.5} \tag{3}$$

where ε_{cs} is the shrinkage coefficient at time t; ε_{cso} is the notional shrinkage coefficient; β_s is the coefficient describing the development of shrinkage with time; t is the age of concrete (days); t_s is the age of concrete (days) at the beginning of shrinkage; h is the notional size of member (mm); t_1 = 1 day; and h_0 = 100 mm.

The creep strain $\varepsilon_{cc}(t, t_0)$ is computed by using the following expression

$$\varepsilon_{cc}(t, t_0) = \frac{\sigma_c(t_0)}{E_{ci}}\phi(t, t_0) \tag{4}$$

$$\phi(t, t_0) = \phi_0\beta_c(t - t_0) \tag{5}$$

where t is the age of concrete (days) at the moment considered; t_0 is the age of concrete at loading (days); E_{ci} is the modulus of elasticity at the age of 28 days; $\phi(t, t_0)$ is the creep coefficient; ϕ_0 is the notional creep coefficient; and β_c is the coefficient of creep with time after loading.

Based on the superposition principle and linear creep assumption, the total strain expression can be expressed as

$$\varepsilon(t) = \frac{\sigma(\tau_0)}{E(\tau_0)}\left[1 + \phi(t, \tau_0)\right] + \int_{\tau_0}^{t} \frac{1}{E(\tau)}\frac{d\sigma(\tau)}{d\tau}\left[1 + \phi(t, \tau)\right]d\tau \tag{6}$$

By setting the incremental creep strain $\varepsilon_c(t) = \varepsilon(t) - \frac{\sigma(\tau_0)}{E(\tau_0)}$, and the incremental creep stress $\sigma_c(t) = \sigma(t) - \sigma(\tau_0)$, assuming that the elastic modulus of concrete is constant: $E = E(\tau_0)$, Eq. (6) can be written as

$$\varepsilon_c(t) = \frac{\sigma(\tau_0)}{E}\varphi(t, \tau_0) + \frac{1}{E}\int_{\tau_0}^{t} \frac{d\sigma_c(\tau)}{d\tau}\left[1 + \varphi(t, \tau)\right]d\tau \tag{7}$$

By applying the integral mean value theorem, Eq. (7) becomes

$$\varepsilon_c(t) = \frac{\sigma(\tau_0)}{E}\phi(t, \tau_0) + \frac{\sigma_c(t)}{E}\left[1 + \rho(t,\tau_0)\phi(t, \tau_0)\right] = \frac{\sigma(\tau_0)}{E}\phi(t, \tau_0) + \frac{\sigma_c(t)}{E_\phi} \tag{8}$$

where E_ϕ is the age adjusted effective modulus and can be written as

$$E_\phi = \frac{E}{1 + \rho(t,\tau_0)\phi(t,\tau_0)} \tag{9}$$

in which $\rho(t, \tau_0)$ is the aging factor which is dependent on the age of loading, the creep function value, and the variation of stress with time. Creep behavior of concrete can be analyzed by combining the above age-adjusted effective modulus method and finite element analysis.

2.3 Master-slave constraint model

There exist two types of assumptions regarding the connection flexibility between the steel girder and concrete slab in a composite section, one is the full bond (Smerda and Kristek 1988, Gilbert 1989, Gilbert and Bradford 1995) (i.e., no slip occurs), and the other is the partial bond (Fragiacomo *et al*. 2004, Ranzi *et al*. 2004, Jurkiewiez *et al*. 2005, Liu *et al*. 2012) (i.e., slip occurs). Design specifications, such as the Eurocode 4 (2005), permit the use of both full and

partial bond systems. In this paper, a full bond is assumed in the subsequent analysis. Based on this assumption, one can use the master-slave constraint method (Jelenić and Crisfield 1986, Muñoz and Jelenić 2006) to simulate the bond. The error in the application of master-slave constraints has been investigated by some researchers (Gupta and Paul 1977, Erkmen *et al*. 2012, Erkmen and Saleh 2012). The master-slave constraints are the conditions imposed such that the displacements of slave nodes depend on those of master nodes. One of the main applications of the master-slave constraints is in modelling floors, which may be considered to be rigid in their own plane in multi-story buildings. In that case, there is one master node at each floor and all other nodes at that floor are slaves.

With respect to steel-concrete composite bridges, the nodes of original finite elements are set as master nodes and the centroidal points of steel and concrete parts are set as slave nodes. Next, the master-slave constraints are applied between the master and slave nodes. Fig. 1 shows the computational model of the master-slave constraints of a steel-concrete composite element. In this figure, the central line of top surface is set as the position of the finite elements and the centroidal points of the steel and concrete parts are set as slave nodes; therefore, a master node is linked with two slave nodes. The master and slave nodes are connected by rigid arms.

Fig. 2 shows the original and displaced positions of master and slave nodes, in which i_c and j_s are the original position of master and slave nodes, i_c' and j_s' are their displaced position due to elastic and rigid body motion of the element. Denoting the coordinates of the master and slave nodes as $i_c(x_i, y_i, z_i)$ and $j_s(x_j, y_j, z_j)$, respectively; the nodal displacements at nodes i and j are $\Delta_i = [u_i\ v_i\ w_i\ \theta_{xi}\ \theta_{yi}\ \theta_{zi}]$, $\Delta_j = [u_j\ v_j\ w_j\ \theta_{xj}\ \theta_{yj}\ \theta_{zj}]$, respectively. Based on the assumption of infinitesimal deformations, the displacement of slave nodes can be obtained from the displacements of the master nodes as (Lv *et al*. 2013)

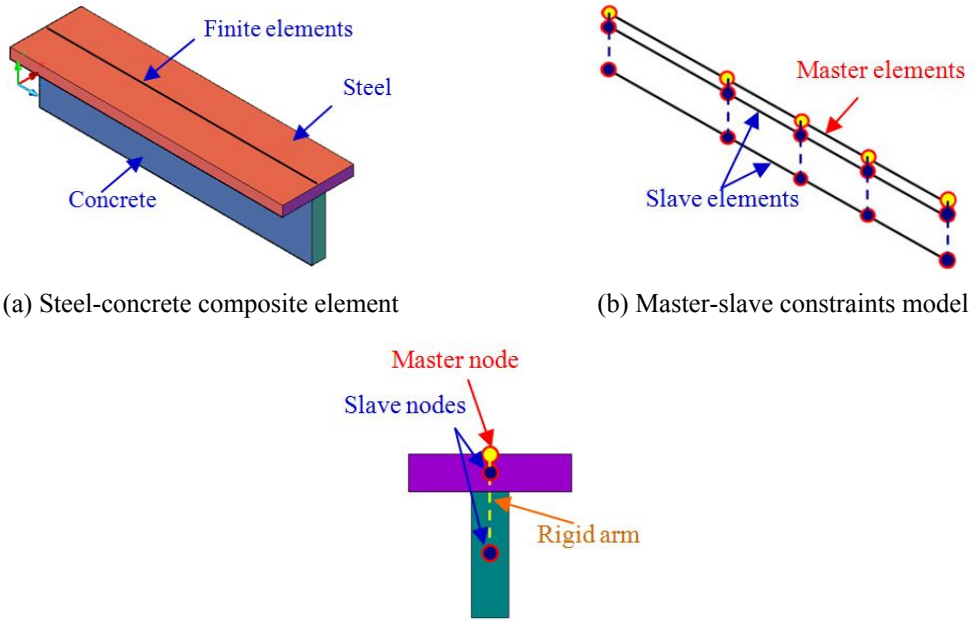

(a) Steel-concrete composite element

(b) Master-slave constraints model

(c) Cross-section

Fig. 1 Computational model of master and slave constraint

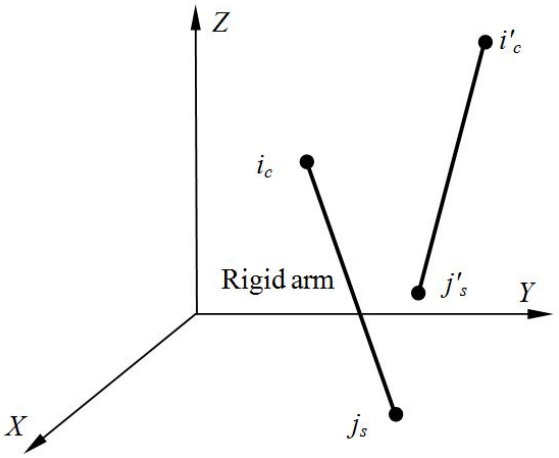

Fig. 2 Original and displaced positions of master and slave nodes

$$\begin{aligned} u_j &= u_i + (z_j - z_i)\theta_{yi} - (y_j - y_i)\theta_{zi} \\ v_j &= v_i + (x_j - x_i)\theta_{zi} - (z_j - z_i)\theta_{xi} \\ w_j &= w_i + (y_j - y_i)\theta_{xi} - (x_j - x_i)\theta_{yi} \\ \theta_{xj} &= \theta_{xi}, \quad \theta_{yj} = \theta_{yi}, \quad \theta_{zj} = \theta_{zi} \end{aligned} \tag{10}$$

Eq. (10) can be expressed in a matrix form as follows

$$[\Delta_j] = [T][\Delta_i] \tag{11}$$

where

$$[T] = \begin{pmatrix} 1 & 0 & 0 & 0 & (z_j - z_i) & -(y_j - y_i) \\ 0 & 1 & 0 & -(z_j - z_i) & 0 & (x_j - x_i) \\ 0 & 0 & 1 & (y_j - y_i) & -(x_j - x_i) & 0 \\ 0 & 0 & 0 & 1 & 0 & 0 \\ 0 & 0 & 0 & 0 & 1 & 0 \\ 0 & 0 & 0 & 0 & 0 & 1 \end{pmatrix} \tag{12}$$

Since the displacements of the slave nodes can be uniquely determined from those of the master nodes, there are no independent degrees of freedom of the slave nodes in the stiffness matrix; therefore, the computation is highly efficient. In the finite element analysis, the effects of master-slave constraints may be substituted by stiff elements whose stiffness is much larger; however, the addition of stiff elements may reduce the accuracy of the analysis and cause computational difficulties due to the large numerical values. Therefore, the master-slave constraint method is desirable for the numerical simulation of steel-concrete composite bridges.

3. The computational tool - SCCB

Based on ObjectARX (2008) and Visual C++, the computational tool SCCB is developed for simulating the construction process of steel-concrete composite bridges. The ObjectARX is a runtime extension programming environment for AutoCAD. Developers can use this environment to develop new AutoCAD applications and commands which operate in the same manner as the built-in AutoCAD commands. The developments based on AutoCAD have the following advantages:

- The development time is significantly reduced since an additional graphical development platform is not required.
- The powerful graphical platform of AutoCAD can be directly used, and a user-friendly interface can be conveniently developed.
- The developed software can be conveniently used by most engineers given the high popularity of AutoCAD.

The ObjectARX applications can be created to take advantage of the Microsoft Foundation Class (MFC) library which allows developers to implement standard user interfaces quickly. A set of classes are provided by the ObjectARX environment to allow developers to create MFC-based user interfaces that behave and appear as the built-in Autodesk user interfaces.

3.1 Main framework of the computational tool

The SCCB tool consists of three main parts: a pre-processing module, an analysis module, and a post-processing module. The main framework of the tool is shown in Fig. 3. The main features of the tool modules are summarized in the following subsections.

3.1.1 Pre-processing module

- Create structural model consisting of elements and nodes from the AutoCAD lines. Since the elements and nodes are inherited from ObjectARX objects, most of the AutoCAD commands, such as copy, erase, move, array, stretch, etc., can be directly used to edit the elements and nodes of the structural model.
- Create, modify or delete cross-section types (e.g., circular, rectangular, I-sections, thin-walled box sections, and composite sections, etc.), material types (e.g., steel and concrete), and creep and shrinkage properties.
- Define group and layer names on the elements and nodes in order to select and display them conveniently.
- Define the construction stages of the bridge. This definition includes activating or deactivating elements, applying loads to elements and nodes, and applying boundary conditions to nodes.
- Define the activated components of the composite steel-concrete cross-sections during the construction stages based on the construction scheme.
- List existing objects and related information, including the index numbers, names, positions, properties of materials and cross-sections, etc.
- Display the index numbers, local coordinates, and loads of elements and nodes.

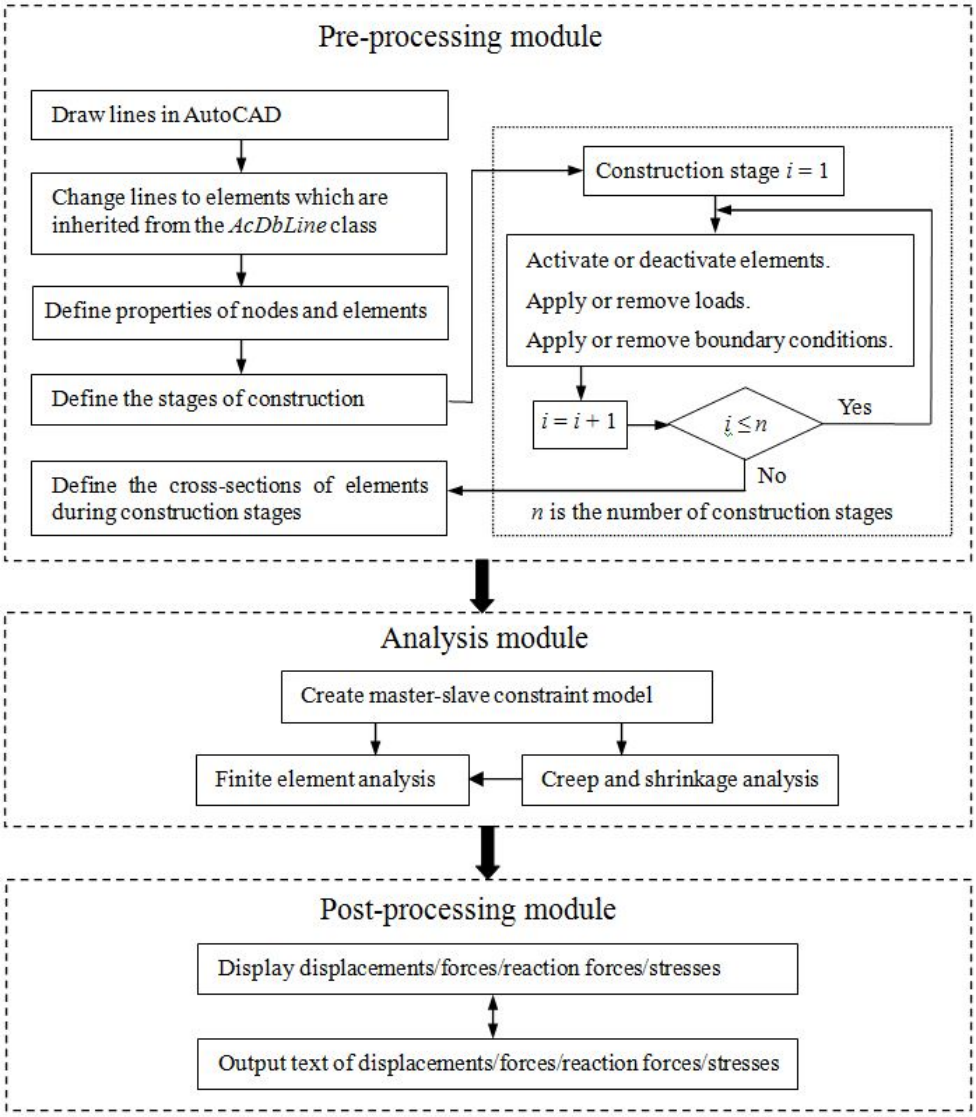

Fig. 3 Main framework of the SCCB tool

3.1.2 Analysis module

- Create the master-slave constraint model based on the definition of construction stages.
- Perform creep and shrinkage analysis.
- Perform 3D finite element analysis.

3.1.3 Post-processing module

- Display the deformed shape of model at each construction stage.
- Display forces/stresses of the steel girders/concrete slabs/composite elements.
- Output text of displacements, forces, stresses, and reaction forces.

3.2 Data structure and main classes

During the past decade, the concept of Object-Oriented Programming (OOP) has been widely applied in the development of structural software (Phongthanapanich and Dechaumphai 2006, Lin *et al*. 2009, Murthy *et al*. 2011). The main features of OOP include data abstraction, data encapsulation, inheritance, and information sharing (Murthy *et al*. 2011). The OOP offers many means of reducing difficulties encountered during the software development life-cycle, and it also helps improving the software code reusability, modifiability, and maintainability (Phongthanapanich and Dechaumphai 2006). The SCCB tool adopts the OOP technique. The major difference between SCCB and other structural software is that the former is based on AutoCAD environment; thus, the structure of SCCB is different from the conventional structural software, especially the pre- and post- processors.

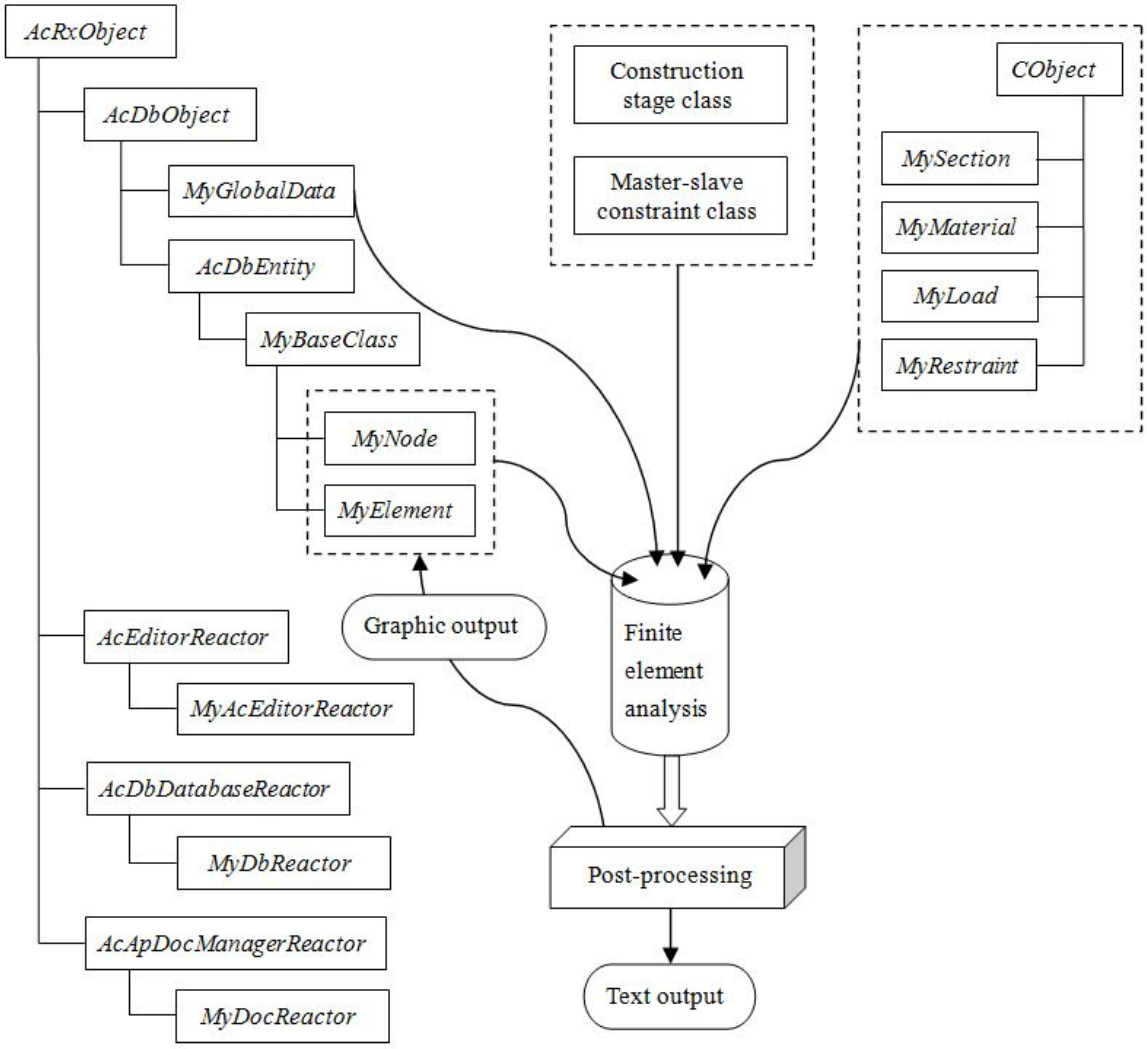

Fig. 4 Main classes and their hierarchy

The main classes and their hierarchy are shown in Fig. 4. The general structure of SCCB consists of several classes that could be classified into three categories: data, graphics, and reactors. The data category consists of several classes containing the structural model. For instance, *MySection* class stores the information of the sectional properties assigned to the elements in the structural model; *MyMaterial* class stores the material properties; *MyLoad* and *MyRestraint* classes are utilized for storing the loads and restraints; and *MyGlobalData* class stores the global variables of the model, such as units of length and weight, scale of text display, and allowable model error, etc.

The graphics category consists of two main classes: *MyElement* class and *MyNode* class, which are the most important classes in the SCCB tool. In fact, they are used not only in the graphics display of geometrical model and calculation results (e.g., display of forces and stresses), but also for the storage of data of the model. The *MyElement* class stores the information of the elements while the *MyNode* class stores all information of the nodes. Some functions of ObjectARX must be loaded to support the AutoCAD commands (e.g., copy, move, stretch, etc).

The reactor category consists of three main classes: *MyAcEditorReactor* class, *MyDbReactor* class, and *MyDocReactor* class, which are inherited from the ObjectARX *AcEditorReactor* class, *AcDbDatabaseReactor* class, and *AcApDocManagerReactor* class, respectively (see Fig. 4). The *MyAcEditorReactor* class is used to manage AutoCAD drawing editor notifications; the *MyDbReactor* class allows notifications to be issued when an object is appended, modified, or erased from a drawing database; and the *MyDocReactor* class provides notifications for a variety of document management events, such as those when the document is created, destroyed, or activated.

3.3 Storage of data

A practical method for data storage is needed due to the potentially large amount of data. Storing all data in the AutoCAD database may result in a very large DWG file which is difficult to manipulate. Therefore, two methods of data storage are adopted in the developed tool: the AutoCAD database and the additional file system. The graphics data (e.g., data of nodes and elements) are stored in Block Tables; and public variables (e.g., unit of length and scale of display) are stored in Named Object Dictionary in AutoCAD database. The additional file system stores data whose quantities are very large, such as calculation results (e.g., displacements, forces and stresses), cross-section library, material library, and load library.

3.4 Finite element analysis

The finite element analysis module of the SCCB tool is a 3D analysis engine. The element library includes: (1) 3D truss element with two nodes; (2) 3D beam-column element with two nodes which can be released to model hinged joints; and (3) 3D link element which can model spring or rigid connections.

Since Eq. (1) needs to be solved iteratively during construction process analysis, the efficiency of the finite element analysis significantly depends on the solution to this equation. For this reason, the sparse matrix algorithm (Duff *et al*. 1986) is adopted to speed up the simulation in the SCCB tool. In this algorithm, only non-zero elements are saved in the total stiffness matrix, and LDL decomposition (Cholesky decomposition) deals with non-zero elements, thus, storage and computational cost are greatly reduced. Detailed description of sparse matrix techniques can be found in Duff *et al*. (1986).

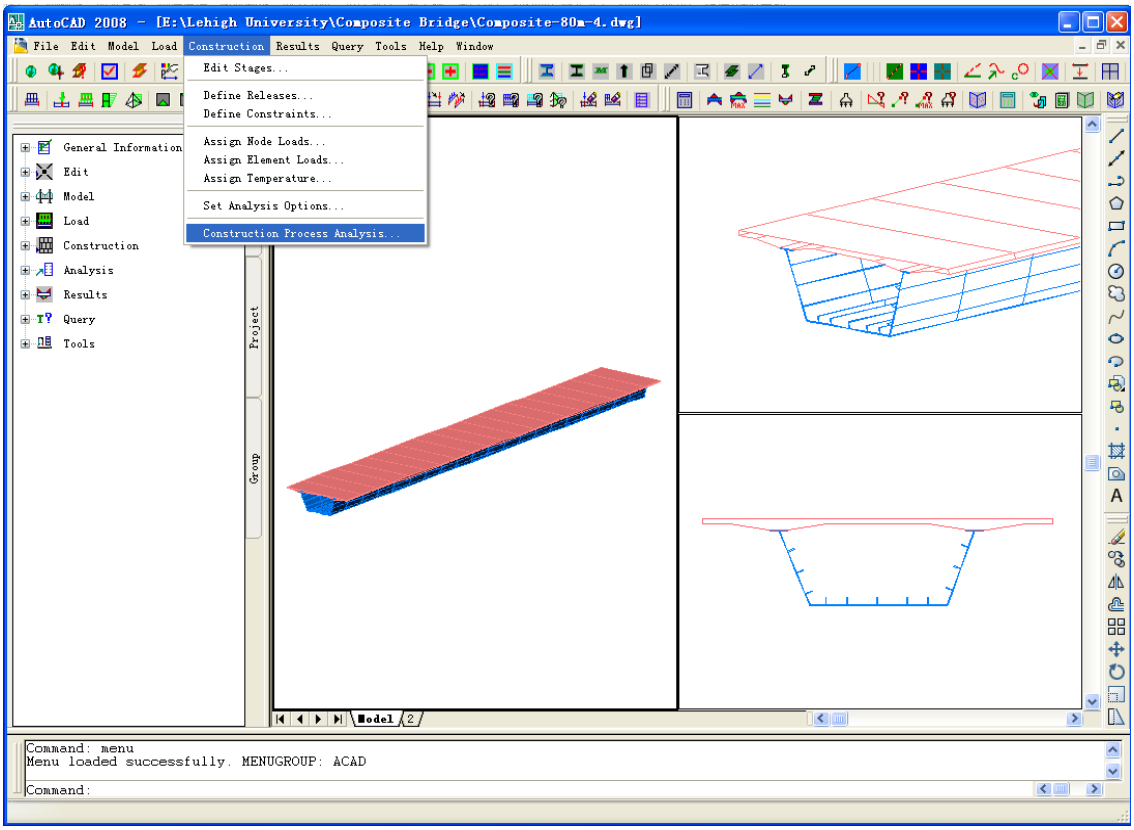

Fig. 5 Main interface of the SCCB tool

3.5 Interface of the computational tool

Fig. 5 illustrates the main interface of the SCCB tool, which consists of top drop-down menus, left tree menus, tool bar, command line, and the graphical interface. Since the developed commands are integrated in AutoCAD environment, the operations on them are very convenient. As described previously, the resisting cross-sections of composite members may change at different construction stages, and the changes must be considered in the construction process simulation. Since the steel and concrete components are divided into separate elements in the master-slave constraint model, their cross-section properties need to be provided individually during the finite element analysis. In order to create and separate the composite cross-sections conveniently, a method of combination of cross-sections is proposed in the developed tool and shown in Fig. 6. In this method, firstly, two cross-sections with a single material (i.e., concrete or steel) are created; secondly, a composite cross-section is formed by linking the two single cross-section regions at accurate position; finally, specific cross-sectional regions are activated during various construction stages. In the SCCB tool, the analysis module automatically changes the composite elements, which are defined by the user, into the master-slave constraint model before executing the finite element analysis (see Fig. 1). After the analysis is completed, the master-slave constraint model is automatically recovered to the original user defined elements. In

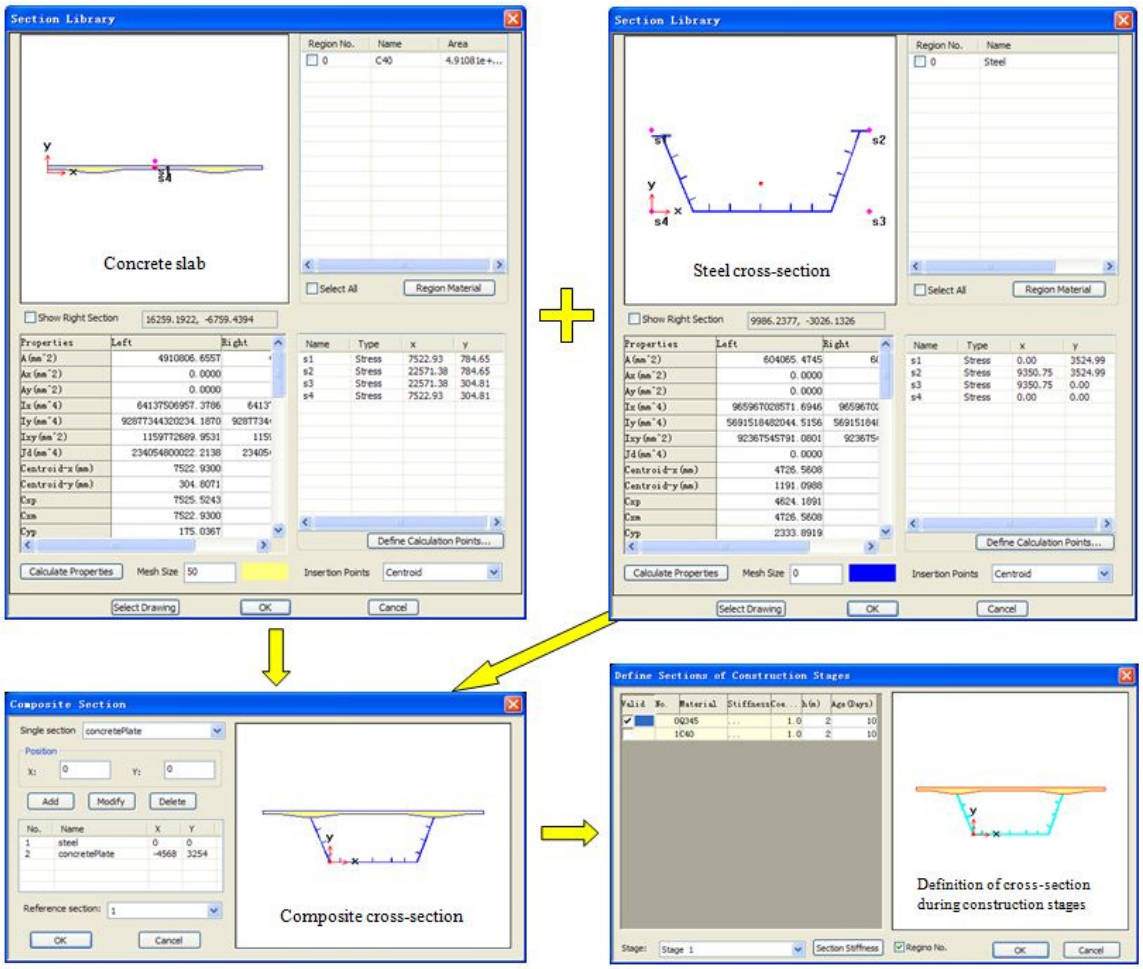

Fig. 6 Interfaces of definition of steel-concrete composite cross-section

other words, the master-slave constraint model is formed by the developed tool itself without needing any further action by the user.

4. Verification and example

4.1 Numerical verification

The developed tool is verified against the results of the transformed-section method example presented in Gilbert (1989). The cross-sectional details are shown in Fig. 7, in which A_{s1} and A_{ss} are the cross-section areas of steel reinforcement and steel I-section, respectively; and I_{ss} is the moment of inertia of steel I-section. The cross-section is subjected to a sustained bending moment M = 450 kNm (the axial force N is zero in this example). The material properties are (Gilbert 1989): E_c = elastic modulus of concrete = 25,000 N/mm^2; E_{s1} = elastic modulus of steel

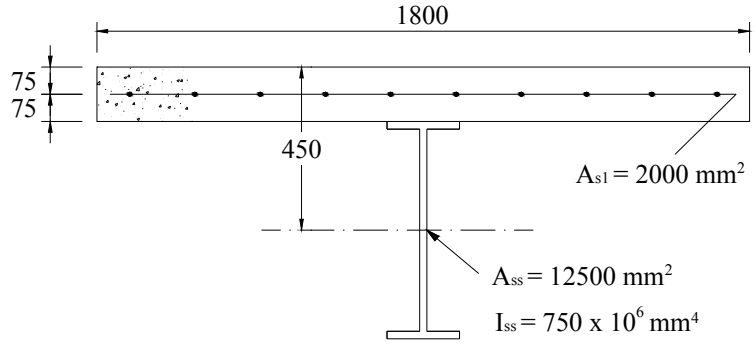

Fig. 7 Cross-sectional details of the verification example (unit: mm; adapted from Gilbert 1989)

Table 1 Comparison between the SCCB tool and manual calculation presented by Gilbert

	Stresses without creep and shrinkage			Stresses considering creep and shrinkage		
	SCCB (N/mm^2)	Gilbert (1989) (N/mm^2)	Errors	SCCB (N/mm^2)	Gilbert (1989) (N/mm^2)	Errors
Top of concrete slab	-4.59	-4.60	0.22%	-1.20	-1.21	0.83%
Bottom of concrete slab	-0.60	-0.60	0.00%	0.81	0.81	0.00%
Top of steel I-section	-4.81	-4.83	0.42%	-102.9	-103.0	0.10%
Bottom of steel I-section	122.9	123.0	0.08%	154.5	154.7	0.13%

reinforcement = 200,000 N/mm^2; E_{ss} = elastic modulus of steel I-section = 200,000 N/mm^2; $\phi(\infty, \tau_0)$ = creep coefficient at time infinity for concrete = 2.5; $\rho(\infty, \tau_0)$ = aging factor at time infinity = 0.8; and $\varepsilon(\infty)$ = shrinkage coefficient at time infinity = 600 × 10^{-6}.

The SCCB tool adopts the CEB-FIP Model (1990) to consider the effects of creep and shrinkage of concrete, the parameters of creep and shrinkage are set as follows: the mean compressive strength of concrete at the age of 28 days is 28 MPa; the relative humidity of the ambient environment is 75%; the notational size of concrete member is 150 mm; the coefficient depending on the type of cement is 8.636; the age of concrete at loading is 16 days; the age of concrete at the beginning of shrinkage is 16 days; and the time of loading is 10,000 days.

In this example, the centroidal line of the steel I-section is set as the position of the finite element, thus, the steel I-girder is set as master element, and the concrete slab and the steel reinforcement are set as slave elements during finite element analysis. The comparison between the SCCB tool and manual calculation presented by Gilbert (1989) is listed in Table 1. The stresses of concrete slab and steel I-section with and without creep and shrinkage are compared. Tensile stresses presented in Table 1 are positive and compressive stresses are negative. As shown in Table 1, the maximum error is within 1.0%, which is reasonable due to numerical approximations.

4.2 Numerical example

Fig. 8 shows a simply supported steel-concrete composite beam bridge with a span of 80 m. The cross-section is composed of a U-shaped open box steel section and a concrete slab, which is

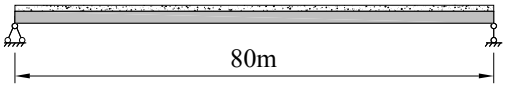

Fig. 8 Simply supported steel-concrete composite beam bridge

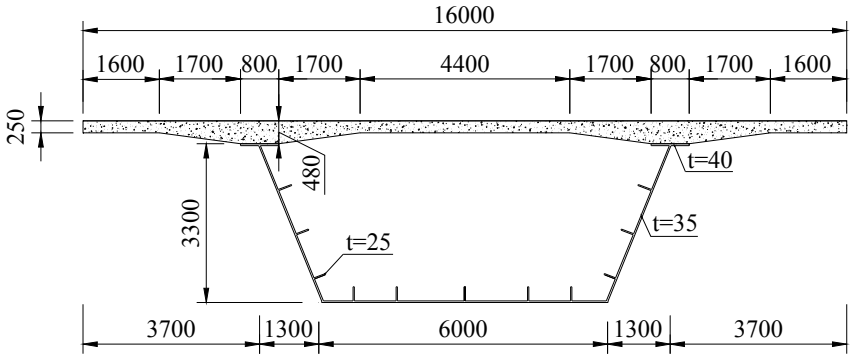

Fig. 9 Cross-section of the bridge (unit: mm)

Table 2 Cross-sections and material properties of steel girder and concrete slab

Property	Notation	unit	Value	
			Concrete slab	Steel girder
Cross-sectional area	A	mm^2	4.911×10^6	6.018×10^5
Moment of inertia	I	mm^4	6.414×10^{10}	9.023×10^{11}
Young modulus	E	N/mm^2	32500	206000
Material density	ρ	kg/m^3	2500	7850
Allowable compressive strength	f_c	N/mm^2	18.4	295
Allowable tension strength	f_t	N/mm^2	1.65	295

shown in Fig. 9. The properties of cross-sections and materials of the steel girder and the concrete slab are listed in Table 2. In order to evaluate the structural effects occurring at different construction stages, two types of construction schemes are considered.The first construction scheme is shown in Fig. 10, in which the construction stages can be described as follows: (a) stage 1: support the steel girder within the span providing a 40 m center span (1 day), to simulate hoisting the steel; (b) stage 2: simply support the steel girder at both ends (1 day), to simulate the installation of the girder on the piers; (c) stage 3: apply uniform load (i.e., 123 kN/m, which is equivalent to the load caused by the weight of the concrete slab) on the steel girder (7 days), to simulate the concrete slab while it is not bonded to the steel girder; (d) stage 4: activate the concrete slab (1 day), to simulate generating the steel-concrete composite action; (e) stage 5: apply secondary dead load (10 days); and (f) stage 6: consider creep and shrinkage during 10 years (3650 days).

The second construction scheme is shown in Fig. 11, and the construction stages can be described as follows: (a) stage 1: support the steel girder (1 day), to simulate hoisting the steel

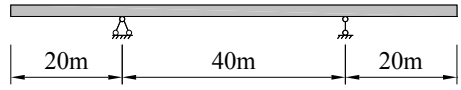

(a) Stage 1

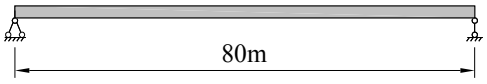

(b) Stage 2

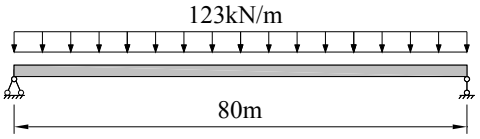

(c) Stage 3

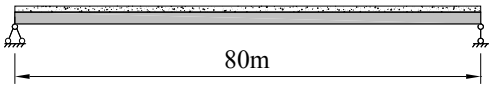

(d) Stage 4

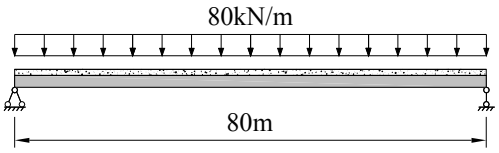

(e) Stage 5

Fig. 10 The construction stages of the first scheme

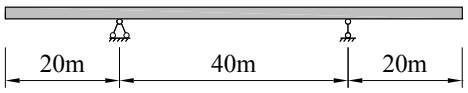

(a) Stage 1

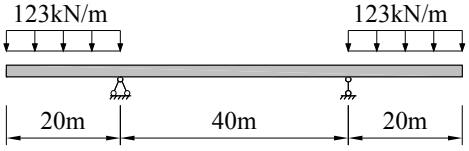

(b) Stage 2

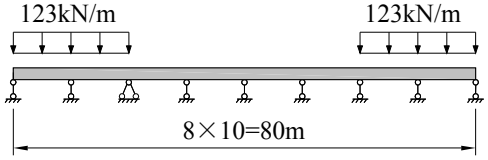

(c) Stage 3

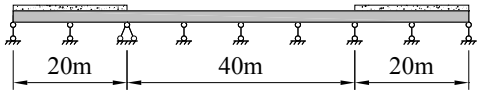

(d) Stage 4

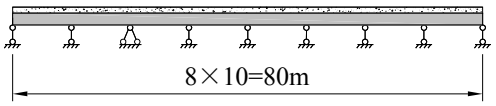

(e) Stage 5

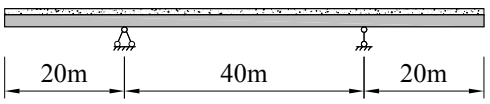

(f) Stage 6

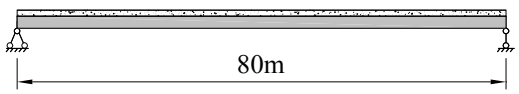

(g) Stage 7

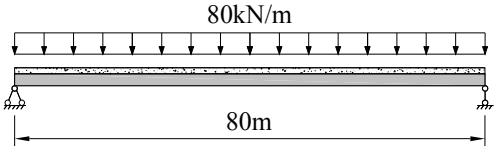

(h) Stage 8

Fig. 11 The construction stages of the second scheme

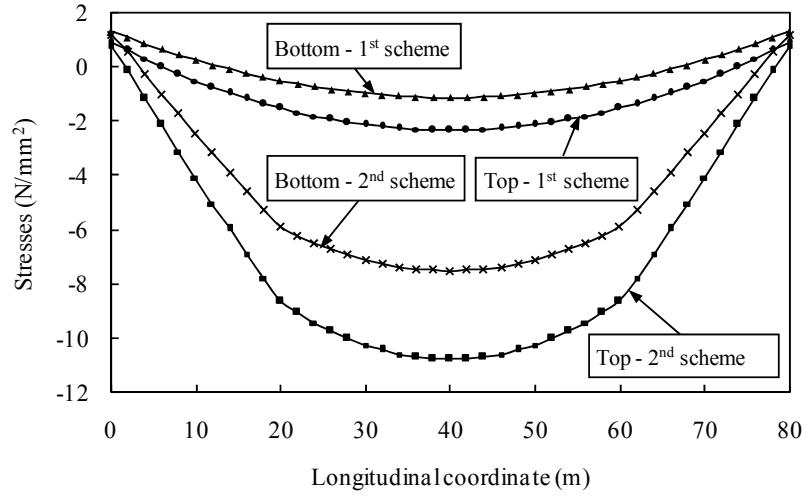

(a) Concrete slab

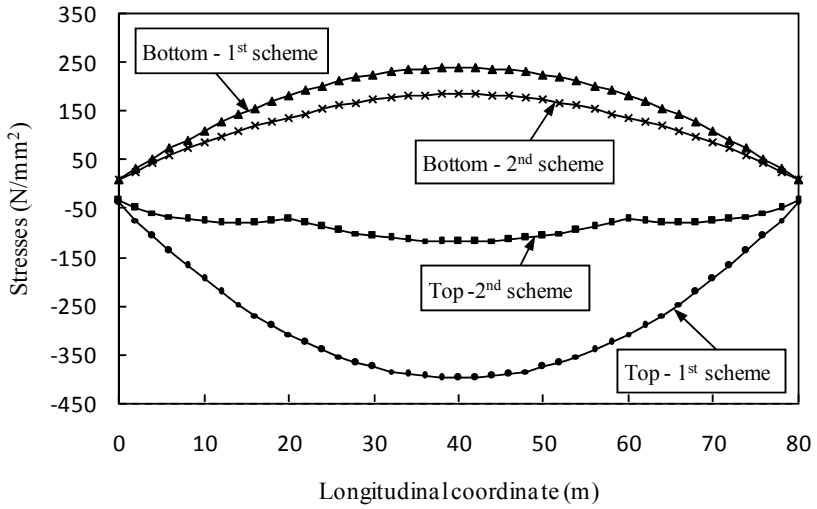

(b) Steel girder

Fig. 12 Stresses at the top and bottom fibers for the first and second schemes

girder onto the precast pedestal; (b) stage 2: apply uniform load on the steel girder within the two cantilever parts (3 days), to simulate the concrete slab while it is not bonded to the steel girder; (c) stage 3: apply vertical restraints at each 10 m interval (1 day), to simulate adding props; (d) stage 4: activate the concrete slab within the two cantilever parts (1 day), to simulate generating the steel-concrete composite action; (e) stage 5: activate the concrete slab within the range of the middle 40 m span (4 days), to simulate generating the whole composite beam; (f) stage 6: support the composite beam at the middle 40 m span (1 day), to simulate hoisting it; (g) stage 7: simply support the composite bridge at both sides (1 day), to simulate installing it on both side piers; (h) stage 8: apply secondary dead (10 days); and (i) stage 9: consider creep and shrinkage during 10 years (3650 days).

In the finite element analysis, the bridge is divided into 40 elements each of 2 m in length (the analysis results indicate that the maximum error of stresses is within 0.5% if the bridge is divided into 80 elements). During the analysis of creep and shrinkage, the mean compressive strength of concrete at the age of 28 days is 40 MPa; the relative humidity of the ambient environment is 70%; the notional size of concrete member is 250 mm; the coefficient depending on the type of cement is 5.0; the age of concrete at the beginning of shrinkage is 5 days. The self-weight of the structure is considered. As the previous subsection, tensile stresses are positive and compressive stresses are negative.

Fig. 12 shows the stresses, for the first and second construction schemes, at the top and bottom fibers of the concrete slab and the steel girder along the longitudinal direction of the bridge at the final construction stage. As shown in Fig. 12, in the first and second schemes, the maximum stresses in the concrete slab are -2.3 N/mm^2 and -10.8 N/mm^2, respectively; and the maximum stresses in the steel girder are -398.7 N/mm^2 and 183.9 N/mm^2, respectively. It is obvious that the second scheme is better than the first one, because, in the first construction scheme, the strength of concrete is not fully utilized while the stress in steel exceeds its allowable limit. As indicated in Fig. 12, the structural behavior of steel-concrete composite bridge can be significantly affected by the construction scheme.

The effects of creep and shrinkage are investigated based on the second construction scheme. Fig. 13 shows the stresses at the top and bottom fibers of the concrete slab and steel girder along the longitudinal direction of the bridge at the final construction stage with and without creep and shrinkage effects. The corresponding maximum stresses are listed in Table 3. As illustrated in this table, with and without creep and shrinkage effects, the maximum stresses in the steel girder are 183.9 N/mm^2 and 161.2 N/mm^2, respectively; and the maximum stresses in the concrete slab are -10.8 N/mm^2 and -14.9 N/mm^2, respectively. It means that the maximum stress in steel girder increases by 14.1%, whereas the maximum stress in concrete slab decreases by 27.5% as a result of creep and shrinkage effects. As indicated in Fig. 13 and Table 3, it can be concluded that creep

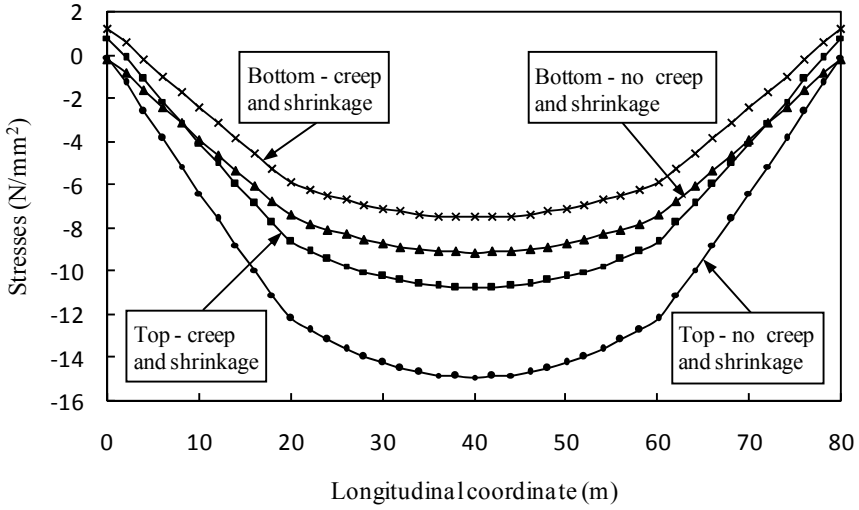

(a) Concrete slab

Fig. 13 Stresses at the top and bottom fibers with and without considering creep and shrinkage

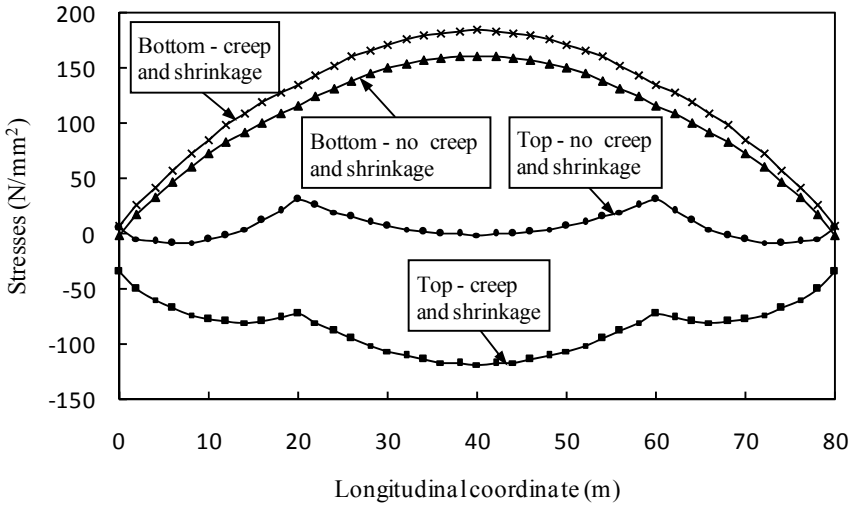

(b) Steel girder

Fig. 13 Continued

Table 3 Comparison of maximum stresses with and without considering creep and shrinkage

	Maximum stresses without creep and shrinkage (N/mm^2)	Maximum stresses considering creep and shrinkage (N/mm^2)	Percentage of stress increase*
Steel girder	161.2	183.9	14.1%
Concrete slab	-14.9	-10.8	-27.5%

and shrinkage have considerable effects on structural behavior of steel-concrete composite bridges.

5. Conclusions

A master-slave constraint method is presented for the construction simulation of steel-concrete composite bridges. The creep and shrinkage of concrete are considered by combining the age-adjusted effective modulus method and finite element analysis. A computational tool SCCB, which is integrated in AutoCAD environment, was developed and applied to the simulation and analysis of steel-concrete composite bridges. The following conclusions are drawn:

(1) The proposed master-slave constraint method may substitute the conventional transformed-section method in the analysis of steel-concrete composite bridges, especially when the construction process, creep, and shrinkage effects are all considered. The major advantage of this method is that it can efficiently handle complex composite cross-sections, which are often difficult to be analyzed by using the transformed-section method.

(2) The developed tool has a user friendly and convenient interface, since it is embedded in AutoCAD environment, most of the AutoCAD commands (e.g., copy, erase, move, stretch, and 3D orbit, etc) can directly edit and modify elements and nodes of the structural model

due to their inheritances from the ObjecARX objects; therefore, the use of the computational tool is very convenient.

(3) The structural behavior of steel-concrete composite bridge can be significantly affected by the construction scheme. Creep and shrinkage have considerable effects on the structural response; therefore, they cannot be neglected in the design of such structures.

(4) The master-slave constraint method described in this paper can be applied for various types of steel-concrete composite elements found in bridges and buildings.

Acknowledgments

This study was carried out when the first author worked as a Visiting Research Scholar at Lehigh University (January 2013-January 2014) in the research group of the second author. The writers would like to gratefully acknowledge the support and cooperation of the Shanghai Tonglei Civil Engineering Technology Co., Ltd., Shanghai, China, especially X.Q. Luo and Q.L. Zhang.

References

ABAQUS (2010), ABAQUS Analysis user's manual (version 6.10); Dassault Systèmes Simulia Corp., Providence, RI, USA.

Amadio, C. and Fragiacomo, M. (1997), "Simplified approach to evaluate creep and shrinkage effects in steel-concrete composite beams", *J. Struct. Eng.*, **123**(5), 1153-1162.

Amadio, C., Fragiacomo, M. and Macorini, L. (2012), "Evaluation of the deflection of steel-concrete composite beams at serviceability limit state", *J. Construct. Steel Res.*, **73**, 95-104.

ANSYS (2012), ANSYS Mechanical user guide (version 14.5); ANSYS Inc., Canonsburg, PA, USA.

Bažant, Z.P. (1072), "Prediction of concrete creep effects using age-adjusted effective modulus method", *ACI J.*, **69**, 212-217.

Bažant, Z.P. (1988), *Mathematical Modeling of Creep and Shrinkage of Concrete*, John Wiley & Sons Ltd., New York, NY, USA.

Bažant, Z.P. (1995), "Creep and shrinkage prediction model for analysis and design of concrete structures-Model B3", *Mater. Struct.*, **28**(6), 357-365.

Bažant, Z.P. (2001), "Prediction of concrete creep and shrinkage: past, present and future", *Nucl. Eng. Des.*, **203**(1), 27-38.

CEB-FIP (1990), CEB-FIP model code 1990: Design code 1994; Thomas Telford, London, UK.

Dezi, L. and Gara, F. (2006), "Construction sequence modelling of continuous steel-concrete composite bridge decks", *Steel Compos. Struct., Int. J.*, **6**(2), 123-138.

Duff, I.S., Erisman, A.M. and Reid, J.K. (1986), *Direct Methods for Sparse Matrices*, Clarendon Press, Oxford, UK.

Erkmen, R.E. and Saleh, A. (2012), "Eccentricity effects in finite element modelling of composite beams", *Adv. Eng. Software*, **52**, 55-59.

Erkmen, R.E., Bradford, M.A. and Crews, K. (2012), "Variational multiscale approach to enforce perfect bond in multiple-point constraint applications when forming composite beams", *Computat. Mech.*, **49**(5), 617-628.

Eurocode 4 (2005), Design of composite steel and concrete structures – Part 2: Rules for bridges; EN1994-2:2005, Brussels, Belgium.

Fragiacomo, M., Amadio, C. and Macorini, L. (2004), "Finite-element model for collapse and long-term analysis of steel-concrete composite beams", *J. Struct. Eng.*, **130**(3), 489-497.

Gardner, N.J. and Lockman, M.J. (2001), "Design provisions for drying shrinkage and creep and

normal-strength concrete", *ACI Mater. J.*, **98**(2), 159-167.
Gilbert, R.I. (1989), "Time-dependent analysis of composite steel-concrete sections", *J. Struct. Eng.*, **115**(11), 2687-2705.
Gilbert, R.I. and Bradford, M.A. (1995), "Time-dependent behavior of continuous composite beams at service loads", *J. Struct. Eng.*, **121**(2), 319-327.
Gupta, A.K. and Paul, S.M. (1977), "Error in eccentric beam formulation", *Int. J. Numer. Method. Eng.*, **11**(9), 1473-1483.
Jelenić, G. and Crisfield, M.A. (1986), "Non-linear master-slave relationships for joints in 3D beams with large rotations", *Comput. Method. Appl. Mech. Eng.*, **135**(3-4), 211-228.
Jurkiewiez, B., Buzon, S. and Sieffert, J.G. (2005), "Incremental viscoelastic analysis of composite beams with partial interaction", *Comput. Struct.*, **83**(21-22), 1780-1791.
Kwak, H.G., Seo, Y.J. and Jung, C.M. (2000), "Effects of the slab casting sequences and the drying shrinkage of concrete slabs on the short-term and long-term behavior of composite steel box girder bridges", *Eng. Struct.*, **23**(11), 1453-1480.
Lin, B.Z., Chuang, M.C. and Tsai, K.C. (2009), "Object-oriented development and application of a nonlinear structural analysis framework", *Adv. Eng. Software*, **40**(1), 66-82.
Liu, X.P., EmreErkmen, R.E. and Bradford, M.A. (2012), "Creep and shrinkage analysis of curved composite beams with partial interaction", *Int. J. Mech. Sci.*, **58**(1), 57-68.
Lv, J., Wu, J., Luo, X.Q. and Zhang, Q.L. (2013), "Time-dependent analysis of steel-reinforced concrete structures", *Struct. Des. Tall Spec. Build.*, **22**(15), 1186-1198.
Mari, A., Mirambell, E. and Estrada, I. (2003), "Effects of construction process and slab prestressing on the serviceability behaviour of composite bridges", *J. Construct. Steel Res.*, **59**(2), 135-163.
Muñoz, J. and Jelenić, G. (2006), "Sliding joints in 3D beams: conserving algorithms using the master-slave approach", *Multibody Syst. Dyn.*, **16**(3), 237-261.
Murthy, A.R.C., Palani, G.S. and Iyer, N.R. (2011), "Object-oriented programming paradigm for damage tolerant evaluation of engineering structural components", *Adv. Eng. Software*, **42**(1-2), 12-24.
ObjectARX (2008), ObjectARX Developer's Guide for AutoCAD 2008; San Rafael, Autodesk Inc.
Pedro, J.J.O. and Reis, A.J. (2010), "Nonlinear analysis of composite steel-concrete cable-stayed bridges", *Eng. Struct.*, **32**(9), 2702-2716.
Phongthanapanich, S. and Dechaumphai, P. (2006), "EasyFEM - An object-oriented graphics interface finite element/finite volume software", *Adv. Eng. Software*, **37**(12), 797-804.
Ranzi, G., Bradford, M.A. and Uy, B. (2004), "A direct stiffness analysis of a composite beam with partial interaction", *Int. J. Numer. Method. Eng.*, **61**(5), 657-672.
Smerda, Z. and Kristek, V. (1988), *Creep and Shrinkage of Concrete Elements and Structures*, Elsevier, Amsterdam, Netherlands.
Tehami, M. and Ramdane, K.E. (2009), "Creep behaviour modelling of a composite steel-concrete section", *J. Construct. Steel Res.*, **65**(5), 1029-1033.

CC